

# SCIENTIFIC REPORTS



OPEN

## Glucocorticoid receptor isoforms direct distinct mitochondrial programs to regulate ATP production

Received: 26 February 2016

Accepted: 25 April 2016

Published: 26 May 2016

David J. Morgan<sup>1,2</sup>, Toryn M. Poolman<sup>2,3,4</sup>, Andrew J. K. Williamson<sup>2,4</sup>, Zichen Wang<sup>5</sup>, Neil R. Clark<sup>5</sup>, Avi Ma'ayan<sup>5</sup>, Anthony D. Whetton<sup>2,4,6</sup>, Andrew Brass<sup>1,7</sup>, Laura C. Matthews<sup>2,8</sup> & David W. Ray<sup>2,3,4</sup>

The glucocorticoid receptor (GR), a nuclear receptor and major drug target, has a highly conserved minor splice variant, GR $\gamma$ , which differs by a single arginine within the DNA binding domain. GR $\gamma$ , which comprises 10% of all GR transcripts, is constitutively expressed and tightly conserved through mammalian evolution, suggesting an important non-redundant role. However, to date no specific role for GR $\gamma$  has been reported. We discovered significant differences in subcellular localisation, and nuclear-cytoplasmic shuttling in response to ligand. In addition the GR $\gamma$  transcriptome and protein interactome was distinct, and with a gene ontology signal for mitochondrial regulation which was confirmed using Seahorse technology. We propose that evolutionary conservation of the single additional arginine in GR $\gamma$  is driven by a distinct, non-redundant functional profile, including regulation of mitochondrial function.

Glucocorticoids (Gc) exert diverse effects on cell fate, energy metabolism, and immune regulation through the glucocorticoid receptor (GR), a member of the nuclear receptor superfamily. In its unliganded state GR is predominantly cytoplasmic, sequestered in a multiprotein complex that includes immunophilins and heat shock proteins. Ligand binding induces a conformational change in the receptor, which is accompanied by rapid post-translational modification of the GR, most notably by phosphorylation. The transformed GR is then released from the multiprotein complex, rapidly translocates to the nucleus and binds to cis-elements to regulate gene expression.

A feature of all nuclear receptors, including GR, is a modular structure comprising an N-terminal modulating domain, a C-terminal ligand binding domain and a central DNA binding domain (DBD). The DBD is critically important for directing sequence specific DNA binding, it lies adjacent to a nuclear localisation signal, and also is an important protein interaction surface, coordinating the recruitment of proteins to GR complexes. Therefore modification of the DBD may alter target gene selection, nucleocytoplasmic shuttling and protein-protein interactions.

GR $\alpha$  is the most abundant isoform, accounting for 90% of GR transcripts across all tissues and is considered the primary mediator of Gc action *in vivo*. The GR $\gamma$  isoform is conserved through mammalian evolution, constituting approximately 10% of GR transcript abundance in all tissues<sup>1,2</sup>, but its specific function remains elusive. GR $\gamma$  was

<sup>1</sup>School of Computer Sciences, University of Manchester, Kilburn Building, Oxford Road, Manchester, UK, M13 9PL.

<sup>2</sup>Faculty of Medical and Human Sciences, University of Manchester, AV Hill Building, Oxford Road, Manchester, UK, M13 9PT. <sup>3</sup>Manchester Centre for Nuclear Hormone Research in Disease, University of Manchester, AV Hill Building, Oxford Road, Manchester, UK, M13 9PT. <sup>4</sup>Manchester Academic Health Sciences Centre, University of Manchester, AV Hill Building, Oxford Road, Manchester, UK, M13 9PT. <sup>5</sup>Department of Pharmacology and Systems Therapeutics, Icahn School of Medicine at Mount Sinai, One Gustave L. Levy Place, Box 1603, New York, NY 10029, USA. <sup>6</sup>Stoller Biomarker Discovery Centre, University of Manchester, Wolfson Molecular Imaging Centre, Palatine Road, Manchester, UK, M20 3LJ. <sup>7</sup>Faculty of Life Sciences, University of Manchester, AV Hill Building, Oxford Road, Manchester, UK, M13 9PT. <sup>8</sup>Faculty of Medicine and Health, University of Leeds, Wellcome Trust Brenner Building, St James's University Hospital, Leeds, UK, LS9 7TF. Correspondence and requests for materials should be addressed to L.C.M. (email: l.c.matthews@leeds.ac.uk) or D.W.R. (email: david.w.ray@manchester.ac.uk)

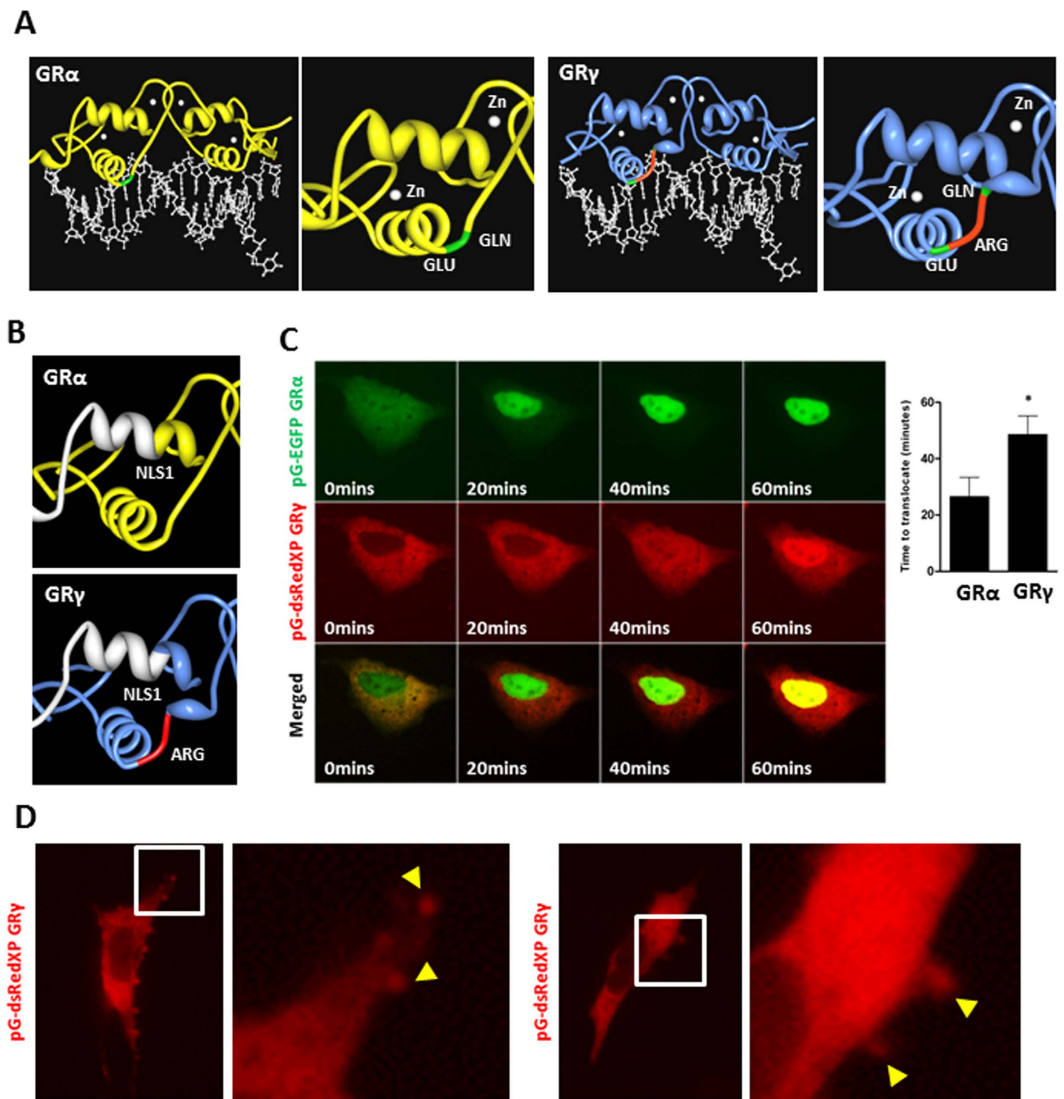


**Figure 1. Kinetics of GR $\alpha$  and GR $\gamma$  activation.** (A) Protein Workshop was used to illustrate conformational differences of GR isoforms bound to FKBP5 promoter (PDB ID 3G6U and 3G6T<sup>8</sup>). GR $\gamma$  (blue) differs from GR $\alpha$  (yellow) by a single arginine residue inserted in the DBD, which is a DNA and protein interaction surface. The additional arginine in the DBD is highlighted in red, with adjacent amino acids shown in green. (B) Protein Workshop was used to illustrate the proximity of the additional arginine to NLS1, shown in white. (C) Cells were co-transfected with pG-EGFP GR $\alpha$  and pG-dsRedXP GR $\gamma$ , cultured in charcoal stripped serum, treated with 100 nM dexamethasone and imaged using time-lapse microscopy. An example of GR $\alpha$  (green) and GR $\gamma$  (red) expression in the same cell is shown. Nuclear translocation from multiples cells were quantified. Graphs (mean  $\pm$  SD) are representative of three independent, and a total of 71 cells were analysed. Samples were compared with an unpaired, two-tailed Student's t test (\* $P < 0.05$ ). (D) Cells were transfected with pG-dsRedXP GR $\gamma$ , cultured in charcoal stripped serum and imaged using time-lapse microscopy. Expanded regions are highlighted with white boxes. Arrows indicate GR $\gamma$  at membrane ruffles.

originally thought to arise from species variation<sup>3</sup>, or mutation<sup>4,5</sup>, but is now recognised to be a constitutive splice variant<sup>2</sup>. In some reports altered GR $\gamma$  expression has been observed in association with altered Gc responses<sup>6,7</sup>.

Alternative splicing between exons 3 and 4, which together encode the DBD, produces the GR $\gamma$  isoform. In fish, alternate exon 3 and 4 splicing incorporates a distinct exon, adding 9 unique amino acids between the two zinc fingers, but in mammals, the GR $\gamma$  isoform has a single additional arginine. Structure-function studies of GR $\gamma$  identified disruption of the lever arm between the two alpha helices (Fig. 1A), and as a consequence an alteration in the DNA sequence binding preference. This results in a difference in the transcriptional regulation of a subset of genes, such as BIRC3 and SDPR, whilst the activation of some genes by GR $\alpha$  and GR $\gamma$ , such as FKBP5, remains similar<sup>8</sup>. These differences are not due to altered DNA binding affinity or GR occupancy at the target genes which suggests that the altered conformation of the lever arm of GR $\gamma$  interprets an allosteric signal from the DNA differently, resulting in a functional effect<sup>8</sup>. Indeed, more recent ChIP-seq studies have demonstrated that GR $\gamma$  has different sequence specificity when compared with GR $\alpha$ <sup>9</sup>.

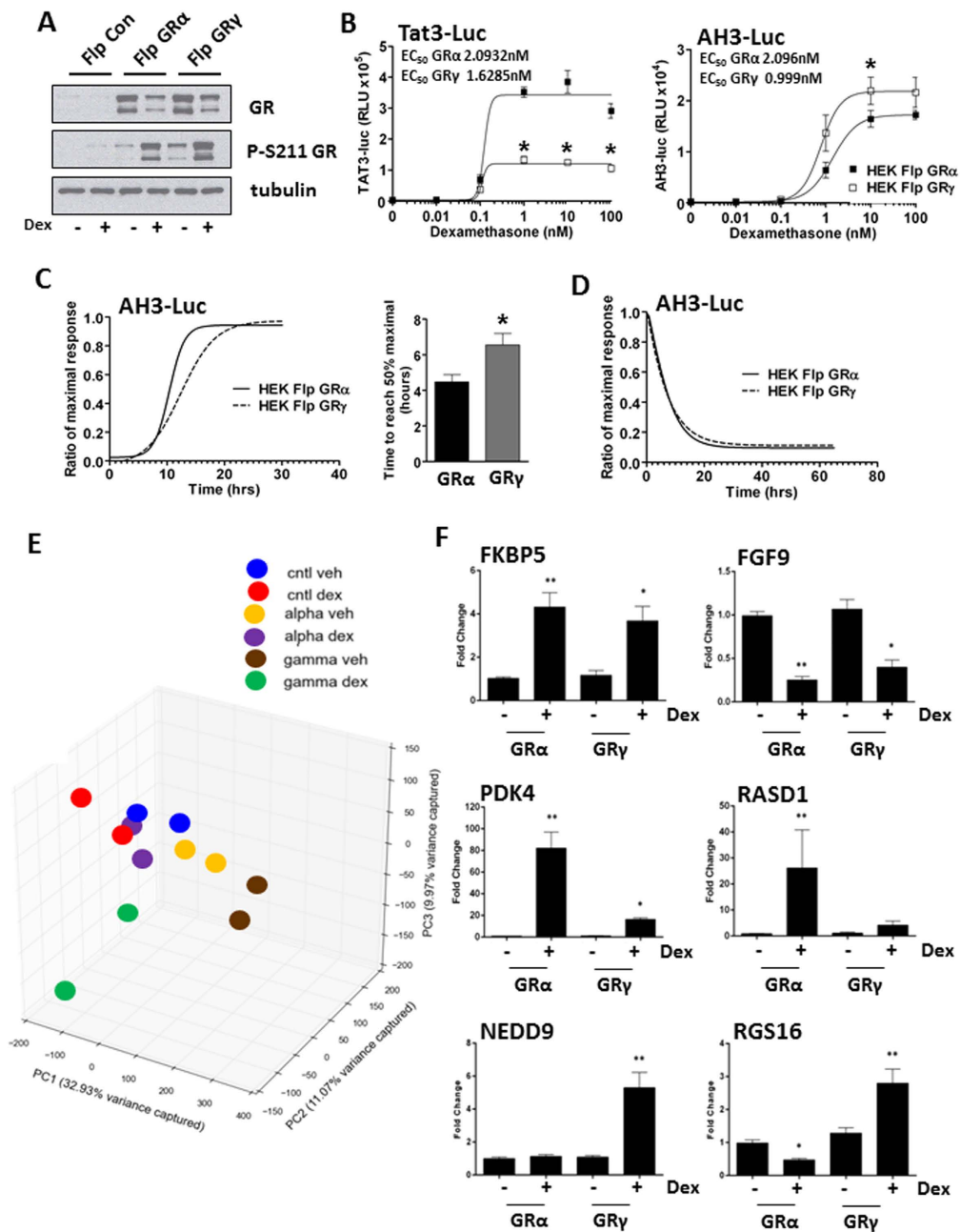


**Figure 2. GR $\alpha$  and GR $\gamma$  transcriptome profiling.** (A) HEK Fip, HEK-FipGR $\alpha$  and HEK-FipGR $\gamma$  cells were treated with 100 nM dexamethasone for 1 hour then immunoblotted for total GR and phosphorylated serine 211 GR. Tubulin is shown as a loading control. (B) HEK-FipGR $\alpha$  and HEK-FipGR $\gamma$  cells were transfected with 2  $\mu$ g of either TAT3-luc or AH3-luc. Cells were treated for 16 hours with varying concentrations of dexamethasone, lysed and then analysed by luciferase assay. EC<sub>50</sub> values are indicated. Samples compared by 2 way ANOVA, (\* $P < 0.05$ ). (C) HEK-FipGR $\alpha$  and HEK-FipGR $\gamma$  cells were transfected with AH3-Luc, treated with 100 nM dexamethasone and the production of luciferase monitored for twenty four hours. Production of luciferase is displayed as a ratio of the maximal response. Graphs (mean  $\pm$  SD) combines data three independent experiments. Samples were compared with an unpaired, two-tailed Student's t test (\* $P < 0.05$ ). (D) Cells from (C) were washed, to remove Gc and the production of luciferase measured for a further 66 hours. HEK Fip, HEK-FipGR $\alpha$  and HEK-FipGR $\gamma$  cells were treated with 100 nM dexamethasone for 4 hours, RNA extracted and duplicate samples subjected to microarray analysis. (E) Principal Component Analysis (PCA) of the gene expression data. Samples profiled by microarray are plotted in the first three principal components space, coloured by condition. Percentages of total variance by each principal component are indicated in the axis labels. (F) HEK-FipGR $\alpha$  and HEK-FipGR $\gamma$  cells were treated with 100 nM dexamethasone for 4 hrs, RNA extracted and analysed by qPCR. Targets regulated by both GR $\alpha$  and GR $\gamma$  (FKBP5, FGF9), or specifically by GR $\alpha$  (PDK4, RASD1) or GR $\gamma$  (NEDD9, RGS16) are shown. Graphs (mean  $\pm$  SD) combine data from three separate experiments and display fold change over vehicle treated control. Stats were performed by one-way ANOVA. Values considered significant when p-value is  $< 0.05$ . \*significant compared to vehicle treated controls, \*\*significant when compared to all samples.

For GR $\gamma$  to be conserved through mammalian evolution it is likely that some positive selective pressure would be required, implying a specific, non-redundant function. Here we define a distinct GR $\gamma$  driven signalling network including identification of GR $\gamma$  specific subcellular trafficking, target gene selection, and engagement of interacting proteins. Both transcriptome, and protein interactome data suggested a role in for GR $\gamma$  in directing mitochondrial function, and indeed GR $\gamma$  expression increased mitochondrial mass, basal respiration, and ATP generation.

## Results

The additional arginine of GR $\gamma$  lies close to the major nuclear localisation signal (NLS1), and may perturb nucleocytoplasmic shuttling (Fig. 1B). To test this, fluorophore tagged GR isoforms were co-expressed. There was a clear difference in isoform distribution, with GR $\gamma$  being more cytoplasmic under ligand-free condition, and showing significantly delayed rates of ligand-induced nuclear import (Fig. 1C, movie S1).

Further live cell analysis revealed striking, organised assembly of the GR $\gamma$  isoform at sites of membrane ruffling, best seen in the accompanying video (Fig. 1D, movie S2). A recent model suggested that nuclear receptors serve as molecular “ferryboats”<sup>10</sup>, which were required to traffic to the plasma membrane in order to become activated. The membrane proximal location of the GR $\gamma$  isoform suggests that this isoform may preferentially respond to lower ligand concentrations and therefore offers an ideal system to test the “ferryboat” theory. However, we found no difference in Gc sensitivity between the GR isoforms (Fig. S1A,B, movie S3).

We next compared overexpression of GR $\alpha$  and GR $\gamma$  in HEK293 cells, which are deficient in endogenous functional GR, using Flp recombinase technology (Fig. S1C). This permitted stable expression of either GR $\alpha$  or GR $\gamma$  with matched integration site and the same level of expression (Fig. 2A). We used the GR isoform specific reporter constructs CGT-luc and KLK3-luc, to confirm the functional acquisition of stable GR $\alpha$  and GR $\gamma$  expressing cells (Fig. S1D). We also found differences in maximal transactivation of two further reporter genes, emphasising the importance of DNA target sequence (Fig. 2B).

As the AH3-luc reporter had similar EC50 and maximal response to both GR isoforms, we used this system to measure transactivation kinetics. GR $\gamma$  transactivation showed a slower onset of transactivation than GR $\alpha$  (Fig. 2C), compatible with the slower rate of translocation, while the decay in transactivation following ligand withdrawal occurred at similar rates for the two isoforms (Fig. 2D).

We next mapped isoform specific Gc targets using gene expression cDNA microarrays. To eliminate effects arising from kinetic differences between the two isoforms, we profiled transcriptomes of GR $\alpha$  and GR $\gamma$  stable FlpIn cells after four hours Dexamethasone treatment.

Principle component analysis (PCA) shows that duplicate samples cluster together, that both GR $\alpha$  and GR $\gamma$  shift global gene expression from the control, and that Dexamethasone treatment induces a shift in global gene expression, with greater change induced by GR $\gamma$  (Fig. 2E). Using the Characteristic Direction method<sup>11</sup> we next identified differentially expressed genes between the control, GR $\alpha$  and GR $\gamma$  cells (Supp. Data File 1) and identified a panel of differentially expressed genes (Figs 2F and S3). Furthermore, we successfully validated these Gc regulated genes in independently derived stable cell lines, and in tetracycline inducible cells (T-RexFlpIn) (Figs S4 and S5).

Enrichment analyses of the differentially expressed genes was performed with Enrichr<sup>12</sup> using the gene set libraries from ENCODE<sup>13,14</sup>, Gene Ontology (GO) cellular component<sup>15</sup>, Wikipathways<sup>16,17</sup> and disease perturbations from GEO<sup>18,19</sup>. This enrichment analysis revealed distinct roles for the two GR isoforms (Supp. Table 1). Genes repressed by GR $\gamma$  had significant overlap with target genes of TCF7L2 (ENCODE, Fisher exact p-value = 3.1e-21) and CTCF (ENCODE, p-value = 2.7e-6) as well as enrichment for triacylglyceride synthesis (Wikipathways, p-value = 5.9e-4). Genes induced by GR $\gamma$  were enriched for components of the mitochondrion (GO\_CC, p-value = 7.5e-4) and linked with the TCA cycle (Wikipathways, p-value = 8.6e-3). Importantly, although GR $\alpha$  and GR $\gamma$  co-regulated some target genes, our transactivated GR $\alpha$ -specific regulated gene set was highly correlated with a previous GR CHIP-seq study (ENCODE, p-values < 1e-8), whereas the GR $\gamma$ -specific regulated gene set did not (Figs 3 and S2), supporting distinct cistromes. These isoform differences are further supported by finding that GR $\alpha$  genes are associated with pulmonary fibrosis and psoriasis (Disease perturbations, p-value = 3.0e-10, 2.2e-12 respectively), while GR $\gamma$  genes associate with cardiomyopathy and Williams-Beuren syndrome (p-value = 2.0e-7, 2.1e-8 respectively, Fig. 3).

Unexpectedly, we also found significant differences in the transcriptional profiles between GR $\alpha$  and GR $\gamma$  in the unliganded state, suggesting a differential ligand-independent role for the two isoforms (Fig. S6A). Although we were able to replicate this finding in independently derived stable FlpIn cell lines, we found no ligand-independent GR $\gamma$  transcripts using T-Rex FlpIn cells (Fig. S6B), suggesting a chronic GR $\gamma$ -dependent cell adaptation, not seen over the shorter time span of tetracycline induction in the TRex system, or confounding induced by tetracycline.

The DBD is an important protein interaction surface (Fig. 4A). To further discriminate between the two isoforms we next considered the protein interactions they engage. We purified GR $\alpha$  and GR $\gamma$  with their putative interacting proteins using a Halo-tag expression system. Using data derived from two independent mass spec (M/S) analyses, we identified a total of 868 GR interacting proteins (Supp. Data File 2). Of these, 67 protein interactions interacted specifically with GR $\alpha$  whereas 253 were specific to GR $\gamma$  (Figs 4B and S7). We identified significant differences between protein partners of the two isoforms. Constitutive interactions were similar between the two isoforms, predominantly heat shock proteins, with correlation to previous low content studies (Fig. S8). The greatest differences in interaction profile were evident in vehicle treated cells with 49 interacting proteins unique to GR $\alpha$  and 218 interacting proteins specific to GR $\gamma$  (Fig. 4B), again a likely reflection of different intracellular distributions in the unliganded state.

Enrichment analysis (Fig. 4C and Supp. Table 1) using datasets from Wikipathways<sup>16,17</sup>, Reactome<sup>20,21</sup> and Gene Ontology (GO) cellular component<sup>15</sup> suggested association of GR $\gamma$  with the electron transport chain and

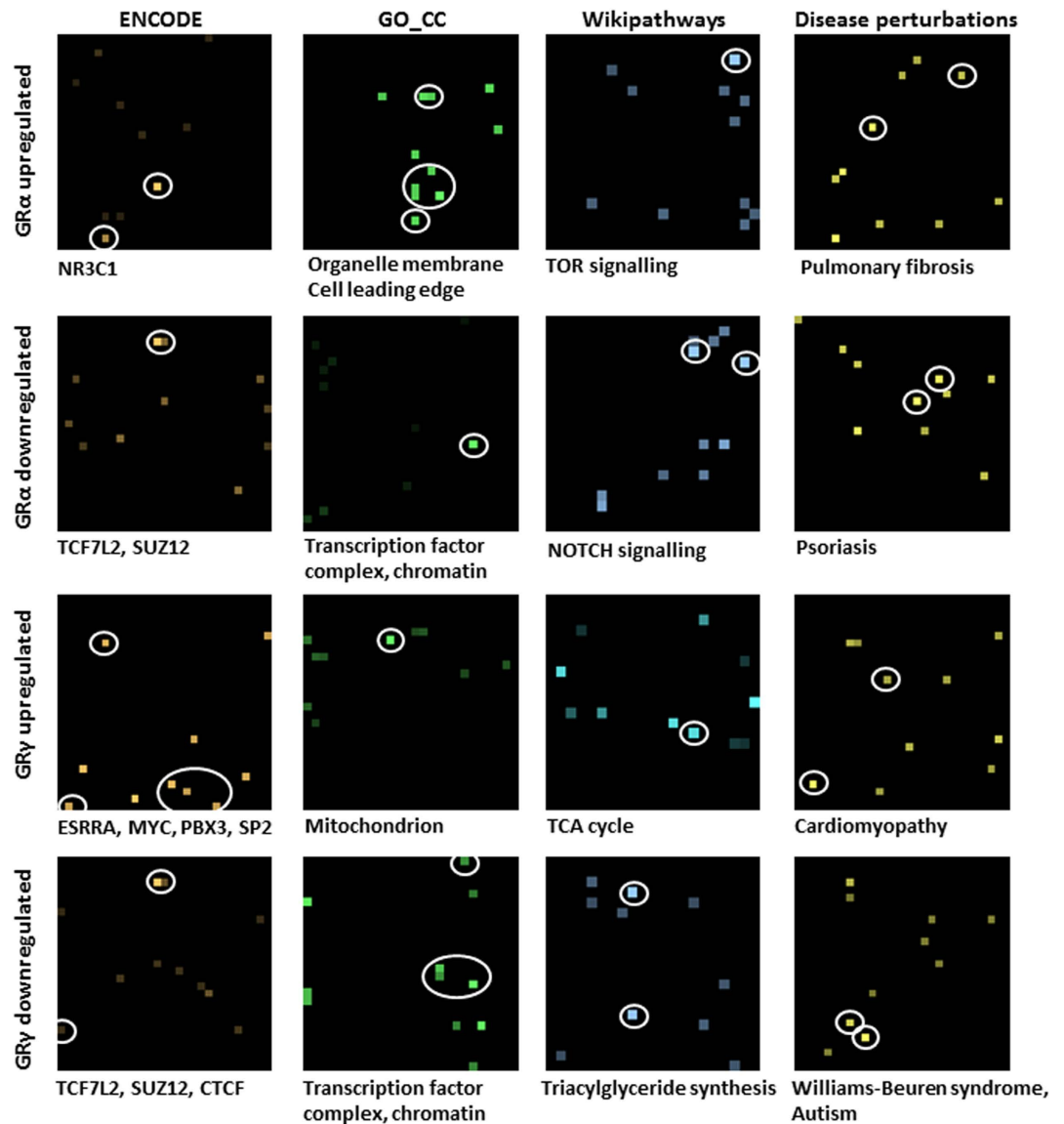


**Figure 3. GR $\alpha$  and GR $\gamma$  transcriptome profiling.** Canvases showing the enriched biological terms for the lists of differentially expressed genes in GR $\alpha$  or GR $\gamma$  cells after activation with Dex (vertical plane). Each canvas represents a specific gene-set library (ENCODE, GO\_CC, Wikipathways, Disease perturbations from GEO), where each square on the canvas represents a single gene set (horizontal plane). The brightness of the squares on the canvases indicates the significance of the enrichment with the gene-set. Squares corresponding to the terms listed underneath each canvas are circled.

oxidative phosphorylation (Wikipathways, p-value = 1.7e-5, 2.8e-3), TCA cycle (Reactome, p-value = 9.4e-5), and components of the mitochondrial membrane (GO\_CC, p-value = 6.8e-10). More detailed analysis of the GR interacting proteins associated specifically with mitochondria revealed shared GR $\alpha$ /GR $\gamma$  and unique GR $\gamma$  mitochondrial-specific interactions (Fig. 4D). This is compatible with the previously reported mitochondrial localisation of GR (<http://www.genecards.org/NR3C1>).

As a mitochondrial signal emerged from both transcriptome and protein interactome datasets, we next analysed mitochondrial morphology, mass, and membrane potential. We discovered significant differences in mitochondrial mass but not membrane potential (although there was a trend), or morphology between GR $\alpha$  and GR $\gamma$  expressing cells (Figs 5A–C, S9 and S10A). Our analysis implied differences in mitochondrial respiration, and so we next investigated this possibility using the Seahorse Xfe analyser (Fig. S10B). In the absence of added ligand, GR $\gamma$  expressing cells have increased basal respiration and ATP production, compared with GR $\alpha$  expressing cells (Fig. 5D), suggesting a specialised role for GR $\gamma$  in regulating mitochondrial function.

## Discussion

The GR $\gamma$  isoform, the result of a constitutive splicing event, is tightly conserved through vertebrate evolution<sup>1,2</sup>. However, with the exception of some reports of altered expression in states of Gc resistance<sup>6,7</sup>, the GR $\gamma$  splice

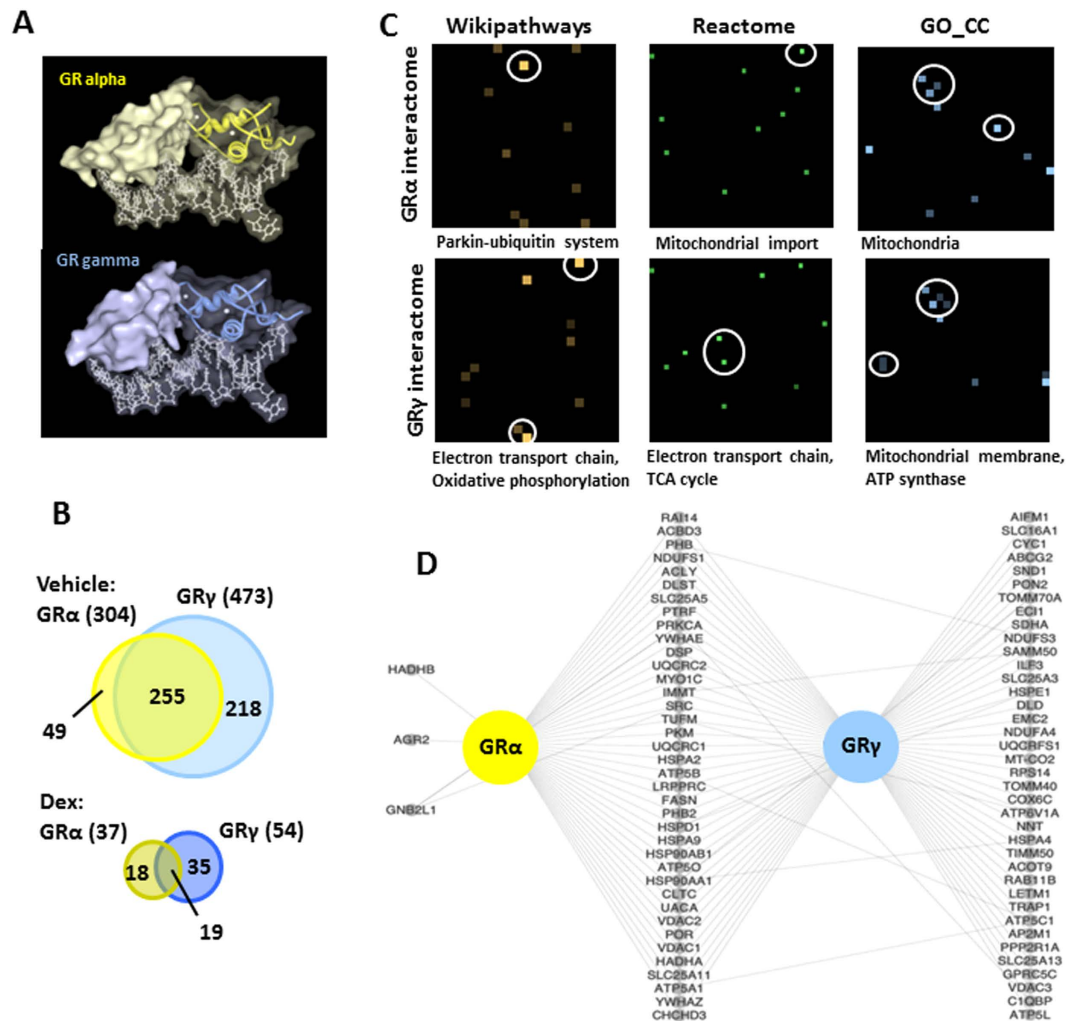


**Figure 4. GR $\alpha$  and GR $\gamma$  interacting proteins.** (A) Protein Workshop was used to generate a partial surface fill of GR isoforms bound to FKBP5 promoter (PDB ID 3G6U and 3G6T<sup>8</sup>). (B) GR $\alpha$  and GR $\gamma$  interacting proteins were determined by proteomics using a HaloTag system. GR $\alpha$  and GR $\gamma$  expressing cells were treated with vehicle or 100 nM dexamethasone for 1 hour, GR-protein complexes purified and determined by MS/MS. Venn diagrams summarise unliganded and liganded GR interactomes. (C) Canvases showing the enriched biological terms for the GR $\alpha$  or GR $\gamma$  identified protein interactions by IP-MS. Each canvas represents a gene-set library (Wikipathways, Reactome, GO\_CC) where each square on the canvas represents a single gene set. The brightness of the squares on each canvas indicates the significance of the enrichment with the gene-set. Squares corresponding to the terms listed underneath each canvas are circled. (D) A network showing the protein interactors identified in this study for GR $\alpha$  or GR $\gamma$  that are also labeled as mitochondria using the GO cellular component ontology.

variant currently lacks the clear, and unique, biological role required to explain its evolutionary preservation. Here we comprehensively define surprising divergence in function conferred by the single additional arginine, and discover a unique biological role for GR $\gamma$ .

GR $\gamma$  takes up a more discretely cytoplasmic localisation than GR $\alpha$ , with striking membrane association, suggesting that GR $\gamma$  may in fact be the elusive membrane GR which has evaded molecular cloning over the past thirty years<sup>22–26</sup>. The membrane association is best appreciated in live cell imaging (movie S2), with clear non-homogeneous, and rapid partition of GR $\gamma$  to dynamically changing plasma membrane locations. The greater cytoplasmic location is accompanied by slower kinetics of nuclear import, suggesting either increased cytoplasmic tethering, or impaired engagement with the nuclear import machinery. Indeed the inserted arginine is close to one of two nuclear localisation sequences (NLS1). The altered compartmentalisation of GR $\gamma$  may contribute to altered kinetics of function. Indeed, the delayed onset of GR $\gamma$  nuclear import was accompanied by a significant delay in transactivation.

Consistent with previous studies, a clear distinction in the pattern of target gene regulation was also seen. The interaction between GR $\gamma$  and DNA recognition sequences has already shown a distinct difference in sequence specificity rather than affinity<sup>8</sup>, and the overlap in target gene expression adds further to this conclusion;

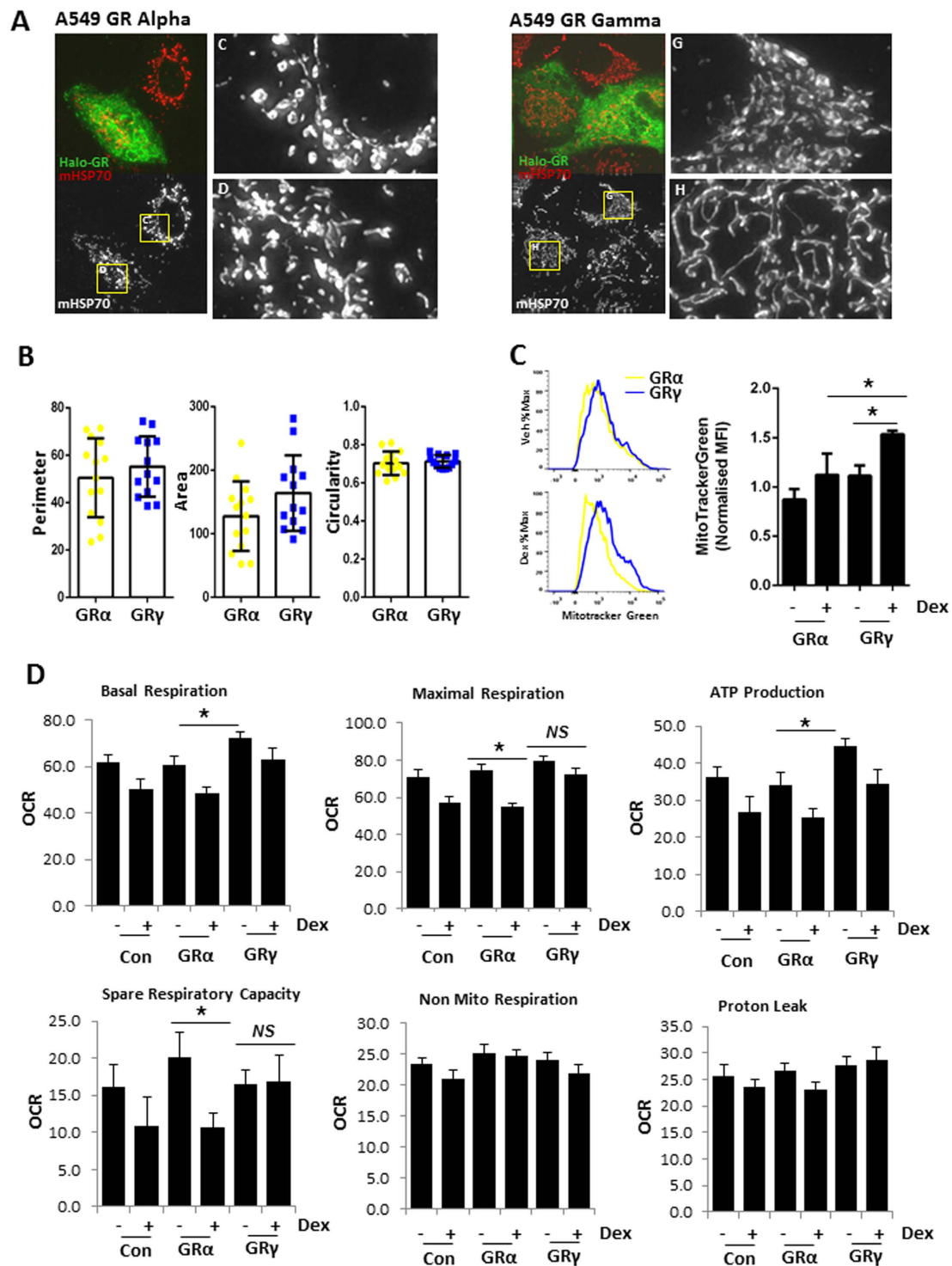


**Figure 5. GR regulation of mitochondrial function.** (A) A549 cells were transfected with 1  $\mu$ g of either HaloTag GR $\alpha$  or GR $\gamma$ , then fixed and immunolabelled with antibodies for HaloTag (green) or mitochondrial HSP70 (red). Higher magnification images of boxed regions are shown inset. Representative images are shown. (B) Mitochondrial morphology (perimeter, area, circularity) was quantified where each individual data point represents an average across a single cell. Data are presented as the mean  $\pm$  SD. (C) HEK-FlpGR $\alpha$  and HEK-FlpGR $\gamma$  cells were treated with 100 nM dexamethasone overnight, then incubated with Mito Tracker Green for 1 hr, and analysed by FACS to measure mitochondrial mass. Shown are representative histograms and quantification of mean fluorescence intensity (MFI) for Mitotracker Green staining. Samples compared with one-way ANOVA, and data presented as the mean  $\pm$  SD of three independent experiments (\* $p$  < 0.05). (D) HEK-FlpGR $\alpha$  and HEK-FlpGR $\gamma$  cells were treated with 100 nM dexamethasone overnight, then mitochondrial function measured on a Seahorse XFe96 analyser. Samples compared with one-way ANOVA, and data presented as the mean  $\pm$  SD of three independent experiments (\* $p$  < 0.05). OCR oxygen consumption rate.

suggesting that binding sites which do not discriminate between GR $\alpha$ , and GR $\gamma$  are similarly regulated by both<sup>9</sup>. Enrichment analysis revealed an intriguing signal of mitochondrial function as distinguishing between the two GR isoforms.

Our discovery of distinct intracellular locations and trafficking kinetics supports GR isoform specific interaction with distinct protein partners, and so we undertook proteomic analysis of GR $\alpha$ , and GR $\gamma$  interactomes under basal, and ligand activated conditions. Significant differences were seen under ligand free conditions, providing a clear correlate to the predominantly cytoplasmic location of the GR $\gamma$  isoform compared to GR $\alpha$ . The cytoplasmic anchoring of GR $\gamma$  may permit or enhance some of these interactions, and other such interactions may contribute to the anchoring, and delayed translocation kinetics. An important distinction was the mitochondrial interactome engaged by GR $\gamma$  in the unliganded state. Localisation of the GR to mitochondria has been reported before<sup>27–31</sup>, but the earlier analyses did not consider GR isoforms. Our new data suggests that these previous observations result in part from the presence of GR $\gamma$ .

Identification of GR $\gamma$  as regulating nuclear genes encoding mitochondrial proteins, and interacting with mitochondrial proteins suggested a coherent biological programme for GR $\gamma$  in regulating cellular energy metabolism. We analysed mitochondrial morphology, and discovered that both GR isoforms reduced mitochondrial circularity, a measure of mitochondrial fusion<sup>32</sup>.

GR $\gamma$  expression resulted in a profound increase in mitochondrial mass, when compared to the GR $\alpha$ . Dynamic energy metabolism was investigated further, using Seahorse technology, which revealed GR $\gamma$  dependent increase in ATP generation, and oxygen consumption. Interestingly, we saw these GR $\gamma$  specific changes in the absence of added ligand. Therefore, our data supports the identity of complementary, but unique, GR isoform actions on mitochondrial energy expenditure. This also provides a mechanism for the transfer of time of day information to the mitochondria through the HPA axis<sup>33,34</sup>. In humans, serum cortisol concentrations are strongly circadian, peaking early morning, falling throughout the day to reach undetectable levels at night. Therefore, at night the ligand independent actions of GR $\gamma$  on mitochondria would be dominant.

We propose that these differential regulatory properties have permitted the evolutionary conservation of GR $\gamma$ . Full characterisation of the physiological role of GR $\gamma$  will require splice site targeting *in-vivo*, but our studies strongly support a unique, and non-redundant role of this isoform in Gc action.

## Materials and Methods

Details of antibodies, plasmids, primers and cells are provided in Supplementary Information.

*Immunoblot analysis*, transfection and reporter gene assays, *quantitative RT-PCR*, *immunofluorescent microscopy*, *live cell microscopy* and *bioluminescent real-time recording* have all been described previously<sup>35,36</sup>.

**Transcriptomics.** HEK-Flp cells were treated with vehicle or dexamethasone for 4 hrs and RNA extracted and processed using an RNeasy kit (Qiagen). RNA quality was established using an Agilent bioanalyser and duplicate samples analysed by microarray using Affymatrix gene array chips.

A list of Gc regulated genes was generated by stratifying duplicate probe sets for the HEK-Flp cells expressing either GR $\alpha$  or GR $\gamma$  compared to the HEK-Flp control cells using the Characteristic Direction method<sup>11</sup>. Functional annotation was performed using Enrichr software<sup>12</sup>. Additional information is provided in Supplementary Information.

**Proteomics.** A549 cells were transfected with GR $\alpha$  or GR $\gamma$  (N-terminal Halo-tag) using polyethyleneimine and treated with vehicle or 100 nM dexamethasone for 1 hour. Cells were lysed, DNase treated and incubated with Halo-link resin overnight (4 °C). The resin was washed 6 times with TBS CA-630, and incubated with 30 units of Tobacco Etch Virus (TEV) protease for 2 hours on ice. Samples were electrophoresed, gels stained with Simply Blue Coomassie safe stain and protein bands were excised, destained and dried overnight at 37 °C. Peptides were extracted and loaded onto an Acclaim Pepmap C18 Trap. Analytical separation of the peptides was performed using Acclaim PepMap100C18 Column on a U3000 RSLC (Thermo). Peptides were separated over a 91 minutes solvent gradient on-line to a LTQ Orbitrap Velos (Thermo). Data was acquired using an information dependant acquisition (IDA) method<sup>37</sup>. Functional annotation was performed using the Enrichr software<sup>12</sup>. Additional information is provided in Supplementary Information.

**Mitochondrial morphology.** A549 cells transfected with GR $\alpha$  or GR $\gamma$  (N-terminal Halo-tag) were stained for Halo-tag and mitochondrial HSP70 as described previously<sup>36</sup>. Mitochondrial morphology was quantified using ImageJ<sup>38</sup>. Deconvolved images were converted into binary images using the default automatic threshold function in ImageJ. Mitochondrial morphology was then quantified, using the built-in ImageJ function Analyze particles to measure the following properties: area, circularity and perimeter.

**Mitochondrial number and membrane potential.** HEK-Flp cells were treated with vehicle or dexamethasone 100 nM overnight, then incubated in 50 ng/ml Mitotracker Green (Life Technologies) for 1 hr at 37 °C to measure mitochondrial mass, or 50 ng/ml TMRM (Life Technologies) for 1 hr at 37 °C to measure mitochondrial membrane potential. Cells were trypsinised and staining assessed by flow cytometry, performed on the BD LSR Fortessa cytometer (BD Biosciences). Data was analysed with FlowJo\_V10 software (Tree Star).

**Mitochondrial stress assays.** HEK-Flp cells were seeded into poly-lysine coated Seahorse culture plates (20 k cells/well) and left to adhere overnight. Cells were treated with vehicle or dexamethasone overnight, then transferred to base media (supplemented with 10 mM Glucose, 1 mM sodium pyruvate and 2 mM glutamine, pH7.4). Mitochondrial stress assays (2  $\mu$ M Oligomycin, 0.5  $\mu$ M FCCP) were performed on a Seahorse XFe96 analyser as per manufacturers instructions. Data was analysed using WAVE.

## References

- Rivers, C., Levy, A., Hancock, J., Lightman, S. & Norman, M. Insertion of an Amino Acid in the DNA-Binding Domain of the Glucocorticoid Receptor as a Result of Alternative Splicing. *J Clin Endocrinol Metab* **84**, 4283–4286 (1999).
- Rivers, C. *et al.* Characterization of Conserved Tandem Donor Sites and Intronic Motifs Required for Alternative Splicing in Corticosteroid Receptor Genes. *Endocrinology* **150**, 4958–4967 (2009).
- Brandon, D. D. *et al.* Genetic variation of the glucocorticoid receptor from a steroid-resistant primate. *J Mol Endocrinol* **7**, 89–96 (1991).
- Ray, D. W., Davis, J. R. E., White, A. & Clark, A. J. L. Glucocorticoid Receptor Structure and Function in Glucocorticoid-resistant Small Cell Lung Carcinoma Cells. *Cancer Res* **56**, 3276–3280 (1996).
- Kasai, Y. Two naturally-occurring isoforms and their expression of a glucocorticoid receptor gene from an androgen-dependent mouse tumor. *FEBS Lett* **274**, 99–102 (1990).
- Haarman, E. G., Kaspers, G. J. L., Pieters, R., Rottier, M. M. A. & Veerman, A. J. P. Glucocorticoid receptor alpha, beta and gamma expression vs *in vitro* glucocorticoid resistance in childhood leukemia. *Leukemia* **18**, 530–537 (2004).
- Beger, C. *et al.* Expression and structural analysis of glucocorticoid receptor isoform gamma in human leukaemia cells using an isoform-specific real-time polymerase chain reaction approach. *Br J Haematol* **122**, 245–252 (2003).
- Meijsing, S. H. *et al.* DNA Binding Site Sequence Directs Glucocorticoid Receptor Structure and Activity. *Science* **324**, 407–410 (2009).
- Thomas-Chollier, M. *et al.* A naturally occurring insertion of a single amino acid rewires transcriptional regulation by glucocorticoid receptor isoforms. *Proc. Natl. Acad. Sci. USA* **110**, 17826–17831 (2013).
- Kolodkin, A. N. *et al.* Design principles of nuclear receptor signaling: how complex networking improves signal transduction. *Mol Sys Biol* **6**, 446 (2010).
- Clark, N. *et al.* The characteristic direction: a geometrical approach to identify differentially expressed genes. *BMC Bioinformatics* **15**, 79 (2014).
- Chen, E. *et al.* Enrichr: interactive and collaborative HTML5 gene list enrichment analysis tool. *BMC Bioinformatics* **14**, 128 (2013).
- ENCODE Project Consortium An integrated encyclopedia of DNA elements in the human genome. *Nature* **489**, 57–74 (2012).
- Rosenbloom, K. R. *et al.* ENCODE whole-genome data in the UCSC Genome Browser: update 2012. *Nucleic Acids Res* **40**, D912–D917 (2012).
- The Gene Ontology Consortium *et al.* Gene Ontology: tool for the unification of biology. *Nat Genet* **25**, 25–29 (2000).
- Kutmon, M. *et al.* WikiPathways: capturing the full diversity of pathway knowledge. *Nucleic Acids Res* **44**, D488–D494 (2015).
- Pico, A. R. *et al.* WikiPathways: Pathway Editing for the People. *PLoS Biol* **6**, e184 (2008).
- Barrett, T. *et al.* NCBI GEO: archive for functional genomics data sets—update. *Nucleic Acids Res* **41**, D991–D995 (2013).
- Edgar, R., Domrachev, M. & Lash, A. E. Gene Expression Omnibus: NCBI gene expression and hybridization array data repository. *Nucleic Acids Res* **30**, 207–210 (2002).
- Croft, D. *et al.* The Reactome pathway knowledgebase. *Nucleic Acids Res* **42**, D472–D477 (2014).
- Milacic, M. *et al.* Annotating Cancer Variants and Anti-Cancer Therapeutics in Reactome. *Cancers (Basel)* **4**, 1180–1211 (2012).
- Gametchu, B. Glucocorticoid receptor-like antigen in lymphoma cell membranes: correlation to cell lysis. *Science* **236**, 456–461 (1987).
- Gametchu, B., Watson, C. S. & Pasko, D. Size and steroid-binding characterization of membrane-associated glucocorticoid receptor in S-49 lymphoma cells. *Steroids* **56**, 402–410 (1991).
- Gametchu, B., Chen, F., Sackey, F., Powell, C. & Watson, C. S. Plasma membrane-resident glucocorticoid receptors in rodent lymphoma and human leukemia models. *Steroids* **64**, 107–119 (1999).
- Matthews, L. *et al.* Caveolin Mediates Rapid Glucocorticoid Effects and Couples Glucocorticoid Action to the Antiproliferative Program. *Mol Endocrinol* **22**, 1320–1330 (2008).
- Trebbles, P. *et al.* Familial Glucocorticoid Resistance Caused by a Novel Frameshift Glucocorticoid Receptor Mutation. *J Clin Endocrinol Metab* **95**, E490–E499 (2010).
- Moutsatsou, P. *et al.* Localization of the Glucocorticoid Receptor in Rat Brain Mitochondria. *Arch Biochem Biophys* **386**, 69–78 (2001).
- Demonacos, C. *et al.* Import of the glucocorticoid receptor into rat liver mitochondria *in vivo* and *in vitro*. *J Steroid Biochem Mol Biol* **46**, 401–413 (1993).
- Scheller, K. *et al.* Localization of glucocorticoid hormone receptors in mitochondria of human cells. *Eur J Cell Biol* **79**, 299–307 (2000).
- Du, J. *et al.* Dynamic regulation of mitochondrial function by glucocorticoids. *Proc. Natl. Acad. Sci. USA* **106**, 3543–3548 (2009).
- Sionov, R. V., Cohen, O., Kfir, S., Zilberman, Y. & Yefenof, E. Role of mitochondrial glucocorticoid receptor in glucocorticoid-induced apoptosis. *J Exp Med* **203**, 189–201 (2006).
- Westrate, L. M., Drocco, J. A., Martin, K. R., Hlavacek, W. S. & MacKeigan, J. P. Mitochondrial Morphological Features Are Associated with Fission and Fusion Events. *PLoS ONE* **9**, e95265 (2014).
- Peek, C. B., Ramsey, K. M., Marcheiva, B. & Bass, J. Nutrient sensing and the circadian clock. *Trends Endocrinol Metab* **23**, 312–318 (2012).
- Peek, C. B. *et al.* Circadian Clock NAD(+) Cycle Drives Mitochondrial Oxidative Metabolism in Mice. *Science* **342**, 1243417 (2013).
- Trebbles, P. J. *et al.* A ligand-specific kinetic switch regulates glucocorticoid receptor trafficking and function. *J Cell Sci* **126**, 3159–3169 (2013).
- Matthews, L. C. *et al.* Glucocorticoid receptor regulates accurate chromosome segregation and is associated with malignancy. *Proc. Natl. Acad. Sci. USA* **112**, 5479–5484 (2015).
- Decaestecker, T. N. *et al.* Information-Dependent Acquisition-Mediated LC-MS/MS Screening Procedure with Semiquantitative Potential. *Anal Chem* **76**, 6365–6373 (2004).
- Schneider, C. A., Rasband, W. S. & Eliceiri, K. W. NIH Image to ImageJ: 25 years of image analysis. *Nat Meth* **9**, 671–675 (2012).

## Acknowledgements

Special thanks to Peter March, Roger Meadows (Manchester Bioimaging) and Gareth Howell (Manchester Flow Facility) for technical assistance and Alan Robinson (MRC Mitochondrial Biology Unit) for advice on the project and proof reading the manuscript. We also thank Sebastiaan Meijsing (Max Planck Institute for Molecular Genetics, Berlin) for kind gifts of CGT-luc and KLK3-luc plasmids. DJM is supported by a BBSRC studentship. AM is supported by NIH grants U54HL127624, U54CA189201, and R01GM098316. ADW and AJKW are supported by Bloodwise. LCM is supported by a FMHS Stepping Stones Fellowship. Bioimaging Facility microscopes used in this study were purchased with grants from BBSRC, Wellcome and the University of Manchester Strategic Fund. The Flow Facility is co-funded by GSK, AZ and the Manchester Collaborative Centre for Inflammation Research.

### Author Contributions

D.W.R. conceived the idea. D.W.R., A.B., A.M., A.D.W. and L.C.M. supervised the project. D.J.M., T.M.P., A.J.K.W. and L.C.M. performed the research. D.J.M., Z.W., N.R.C., A.M. and A.B. analysed the data. D.J.M. L.C.M. and D.W.R. wrote the manuscript. D.J.M. and L.C.M. prepared the figures. All authors reviewed the manuscript.

### Additional Information

**Supplementary information** accompanies this paper at <http://www.nature.com/srep>

**Competing financial interests:** The authors declare no competing financial interests.

**How to cite this article:** Morgan, D. J. *et al.* Glucocorticoid receptor isoforms direct distinct mitochondrial programs to regulate ATP production. *Sci. Rep.* **6**, 26419; doi: 10.1038/srep26419 (2016).



This work is licensed under a Creative Commons Attribution 4.0 International License. The images or other third party material in this article are included in the article's Creative Commons license, unless indicated otherwise in the credit line; if the material is not included under the Creative Commons license, users will need to obtain permission from the license holder to reproduce the material. To view a copy of this license, visit <http://creativecommons.org/licenses/by/4.0/>